Chapter 3

Degradation of the Microstructure and Mechanical Properties of High-Chromium Steels Used in the Power Industry

Grzegorz Golański, Cezary Kolan and Joanna Jasak

Additional information is available at the end of the chapter

http://dx.doi.org/10.5772/intechopen.70552

Abstract

High-chromium martensitic steels are one of the basic creep-resisting construction materials used for the modernization of old and the construction of new power units. During the service under creep conditions, the metastable microstructure of martensitic steels undergoes gradual degradation. The rate of degradation mostly depends on the operating temperature, but it is also affected by stresses. The changes in the microstructure of martensitic steels have an influence on the decrease in their mechanical properties, including creep resistance. The knowledge and description of the changes in the microstructure of steels working under creep conditions allow extending the time of safe operation of the elements of power systems. The paper presents and describes the main mechanisms of degradation of 9–12%Cr martensitic steels on the basis of the independent studies and literature data.

Keywords: creep-resistant steel, 9–12%Cr steel, microstructure degradation, precipitates, mechanical properties

1. Introduction

The need to reduce emissions of pollutants (mainly CO_2) to the atmosphere enforced by increasingly stringent EU directives has contributed to the development of conventional energy. Restrictions on emissions to the atmosphere caused by the combustion of fossil fuels have forced the power industry to increase the thermal efficiency of power units (from 33–35 to 40%, and ultimately up to 50%). On the other hand, the need to increase the thermal efficiency of power units involves a significant increase in steam parameters (pressure, temperature). This

requires the construction of new and the modernization of existing power units to allow them to operate at the so-called supercritical or ultra-supercritical steam parameters. The increase in steam parameters in new and existing power units was possible due to the materials revolution in the power industry and was associated with the introduction of new grades of steels and cast steels with higher resistance to creep and oxidation than that of the materials used so far. The implementation of new materials in the power industry took place primarily through modifications and optimizations of steels that were already being used in the power sector. It has contributed not only to the increase in steam parameters, but also to the reduction in overall dimensions of boiler components, and thus in their weight, which has also a significant impact on the reduction in the energy production costs [1, 2].

One of the new steel groups introduced to the power industry was high-chromium martensitic steels containing 9–12%Cr. By the optimization of carbon content and the introduction of additions and micro-additions such as W, Co, V, Nb, N, B, and Cu to these steels, the construction materials characterized by high mechanical properties were obtained. For example, their creep strength is higher by approx. 20–25% than that of the steels used so far [2, 3]. The expected high reliability and long life of up to a minimum of 200,000 h of pressure parts made from, among others, 9–12%Cr steels require understanding and describing the effects and microstructure degradation processes for these materials. Based on many years of Authors' own research and literature data, the main steel/martensitic cast steel microstructure degradation mechanisms and their impact on mechanical properties were described and characterized in this paper.

2. Microstructure degradation and properties of 9–12%Cr steels

The basic requirement for creep-resistant steels used in the broadly understood power industry is to maintain—for a relatively long time of operation (at present, 200–250,000 h)—the assumed mechanical properties at the operating temperature of power equipment components. The maintenance of the required mechanical properties of creep-resistant steels during long-term service depends on the stability of their microstructure. The structural components of the power equipment are influenced by the continuous destruction process, which has a significant impact on the life and time of safe service of a specific component. Therefore, the time of safe service for devices used in the power industry is one of the most important parameters related to their life, and it determines their applicability in this sector [1, 4, 5].

During their long-term service, progressive changes in microstructure of creep-resistant steels take place—the process of degradation of their microstructure occurs. For 9–12%Cr martensitic steels, the main microstructure degradation mechanisms include [6–8]:

- matrix recovery and polygonization processes,
- coagulation of $M_{23}C_6$ carbides,
- precipitation of secondary phases: Laves phase and Z-phase, and
- depletion of alloying elements in matrix.

http://dx.doi.org/10.5772/intechopen.70552

Martensitic steels in the hardened condition are characterized by high dislocation density within the martensite laths (10^{16}–10^{18} m^{-2}). Due to high-temperature tempering of hardened steel, a more thermodynamically stable microstructure with still high dislocation density at 10^{12}–10^{14} m^2 (including free dislocations) within the subgrains formed during the tempering is obtained. The dislocation substructure in 9–12%Cr steels is characterized by small elongated subgrain (of 200–400 nm in width) and low-angle boundaries [6, 7, 9, 10]. High dislocation density and microstructure refinement with dislocation boundaries has a very intensive impact on the 9–12%Cr steel hardening with the dislocation hardening mechanism and the grain boundary hardening mechanism, respectively. The calculations in [11] showed that the gain in yield strength in martensitic steels for the above-mentioned mechanisms is 18 and 33%. In addition to this hardening, the following further mechanisms are additionally used to form the structure and mechanical properties of 9–12%Cr steels: solution hardening with interstitial and substitution elements and precipitation hardening [9, 11, 12]. In high-chromium martensitic steels, the precipitation hardening mechanism is mainly performed by the secondary particles precipitated when tempering $M_{23}C_6$ carbides and MX precipitates. In 9–12%Cr creep-resistant steels, three types of MX precipitates can occur [3, 13, 14]:

- Primary niobium-rich spheroidal NbC carbides (carbonitrides)
- Secondary lamellar VN (VX) nitrides (carbonitrides), which are precipitated within the martensite laths during high-temperature tempering
- Precipitate complexes consisting of the spherical NbX precipitate in which the VN precipitate nucleates, referred to as the "V-wings"

The degree of hardening with secondary phase precipitates depends mainly on the amount and size of precipitates and their distribution within the matrix.

High-chromium martensitic steels in the as-received condition (i.e., after quenching and tempering) have a metastable microstructure, which will be affected by gradual evolution as a result of long-term service (**Figure 1**).

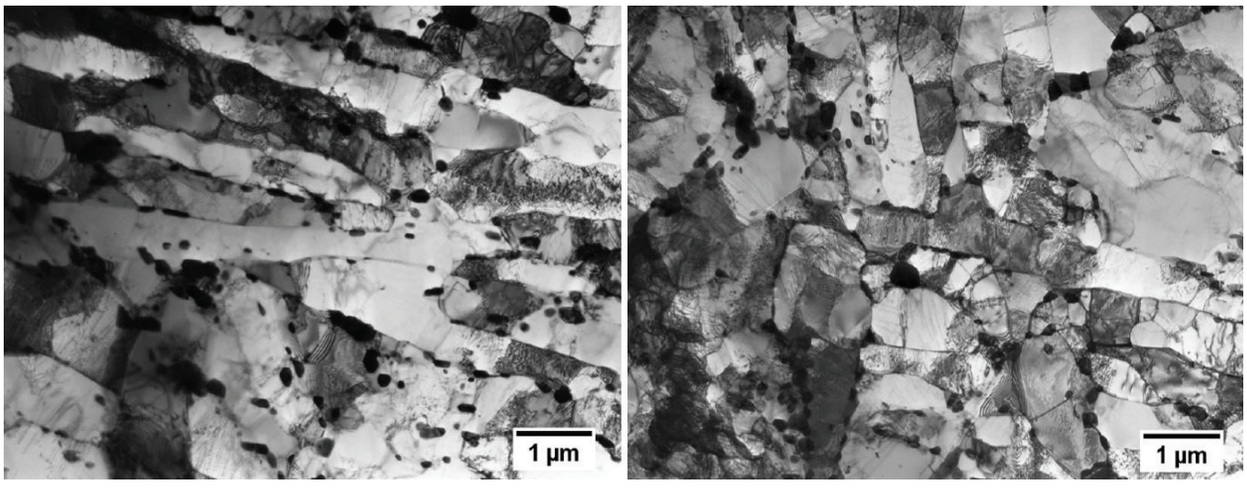

Figure 1. The microstructure of GP91 cast steel in the as-received condition [8].

Long-term effect of the temperature and time, in the case of creep as well as stress, leads to a decrease in strengthening with the dislocation mechanisms and the grain boundaries. A decrease in free dislocation density within grains and increase in size of the subgrains take place. The decrease in dislocation density with the time of service/aging is associated with the progressing process of their regrouping, arranging, annihilation, and entangling the dislocations in grain boundaries as well as the formation of cellular dislocation and subgrain microstructure (**Figure 2**). The matrix recovery and polygonization process results in the disappearance of martensite lath microstructure and the formation of polygonised ferrite microstructure **Figures 3** and **4**.

In the microstructure of martensitic steels, the formation of polygonal structure during service takes place due to the progressive increase in the size of subgrains. This process is slow because of low mobility of these subgrains. The stability of subgrain size has a positive impact on the maintenance of high mechanical properties, including creep resistance [16]. The increase in the size of subgrains occurs due to the migration or coalescence of the sub-boundaries.

The increase in the size of sub-boundaries usually takes place with the "Y" mechanism [15, 17, 18]. The migration with this mechanism is based on the movements of "Y" nodes that are the place where three sub-boundaries meet, which allows the coalescence of two low-angle boundaries. The increase in the size of subgrains with the "Y" node movement mechanism is shown in **Figure 5**.

The matrix recovery and polygonization process takes place in the presence of secondary dispersion phases, which act as a stabilizing agent. The lath microstructure stability depends on the stability of $M_{23}C_6$ carbides precipitated on these phases (**Figure 6**). $M_{23}C_6$ carbides precipitate on the tempered martensite lath boundaries and on the subgrain boundaries preventing

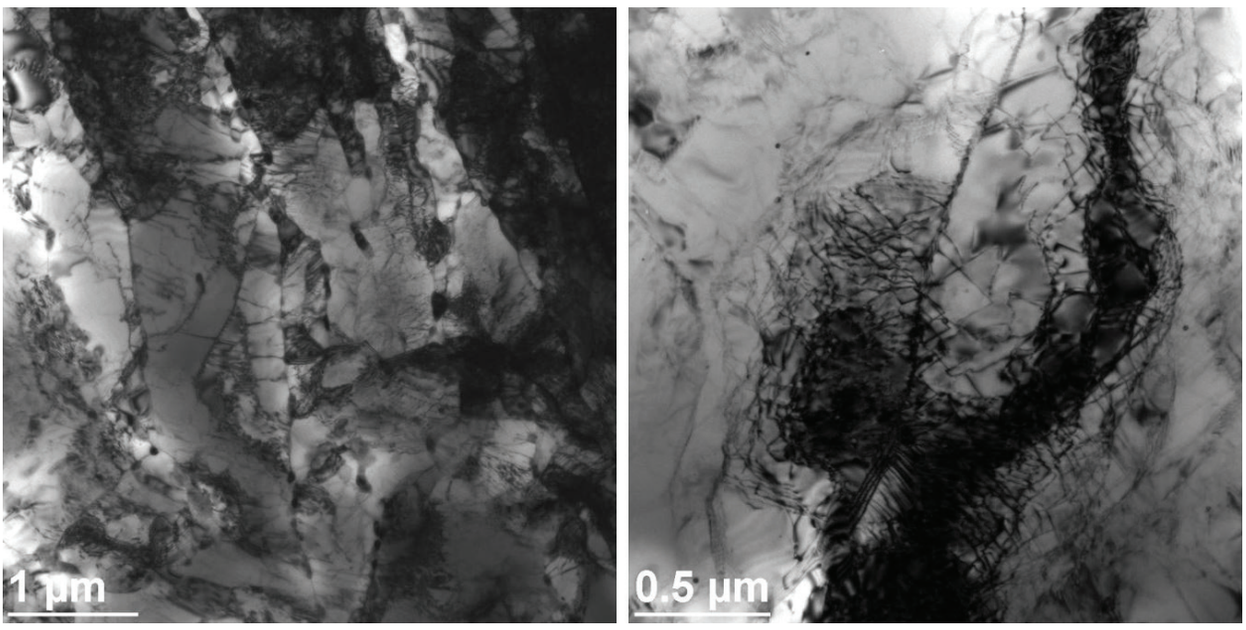

Figure 2. The interaction of dislocations with lath/subgrain boundaries, PB2 steel, TEM.

http://dx.doi.org/10.5772/intechopen.70552

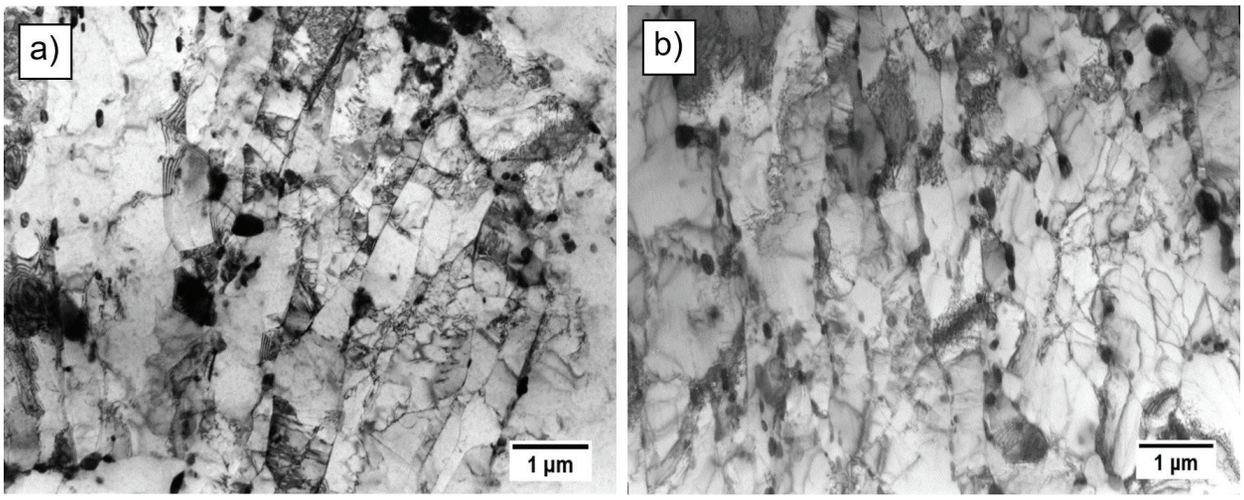

Figure 3. The microstructure of: (a) T91 steel after long-term service [12], (b) GP91 cast steel after 70,000 h aging at 600°C.

their growth due to the matrix polygonization, repolygonization, and recrystallization processes [17, 19]. In addition, the elongated shape of $M_{23}C_6$ carbides precipitated on the subboundaries (**Figures 1**, **3**, and **5**) has a positive impact on anchoring the boundaries by them as their contact surface with the boundary on the same volume fraction is bigger than for spherical particles [18].

The thermodynamic thermal stability of $M_{23}C_6$ carbides is not too high—the $Cr_{23}C_6$ carbide formation enthalpy is: –20 kJ/mol [20]. In the as-received condition, the size of $M_{23}C_6$ carbides

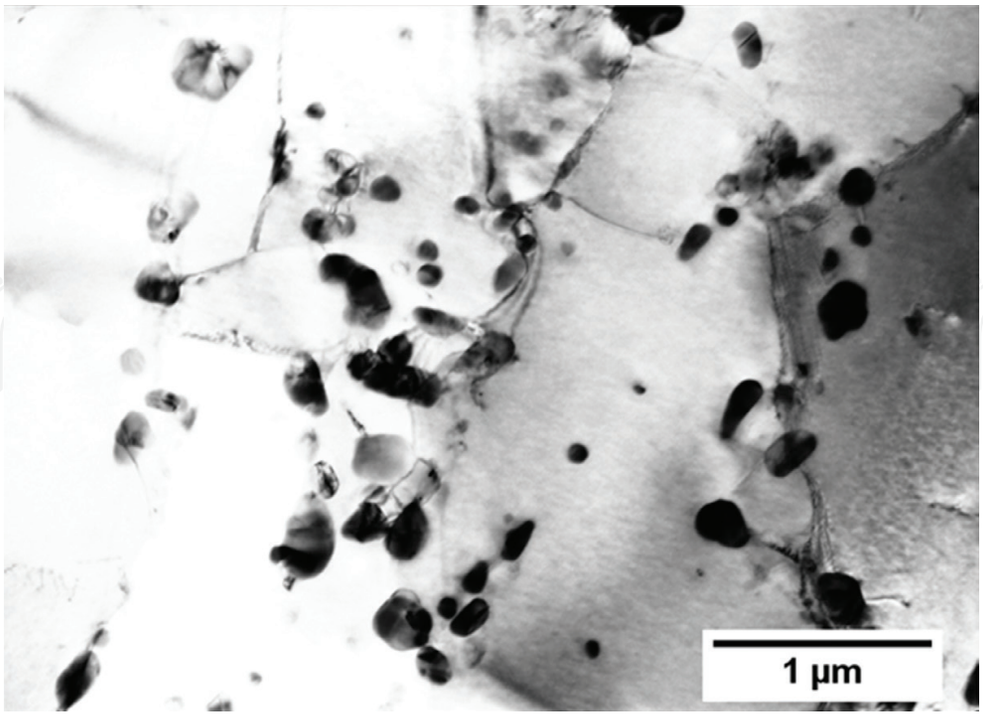

Figure 4. The microstructure of polygonised ferrite with numerous precipitates in GP91 cast steel after low-cycle fatigue at 600°C with strain amplitude of 0.60%.

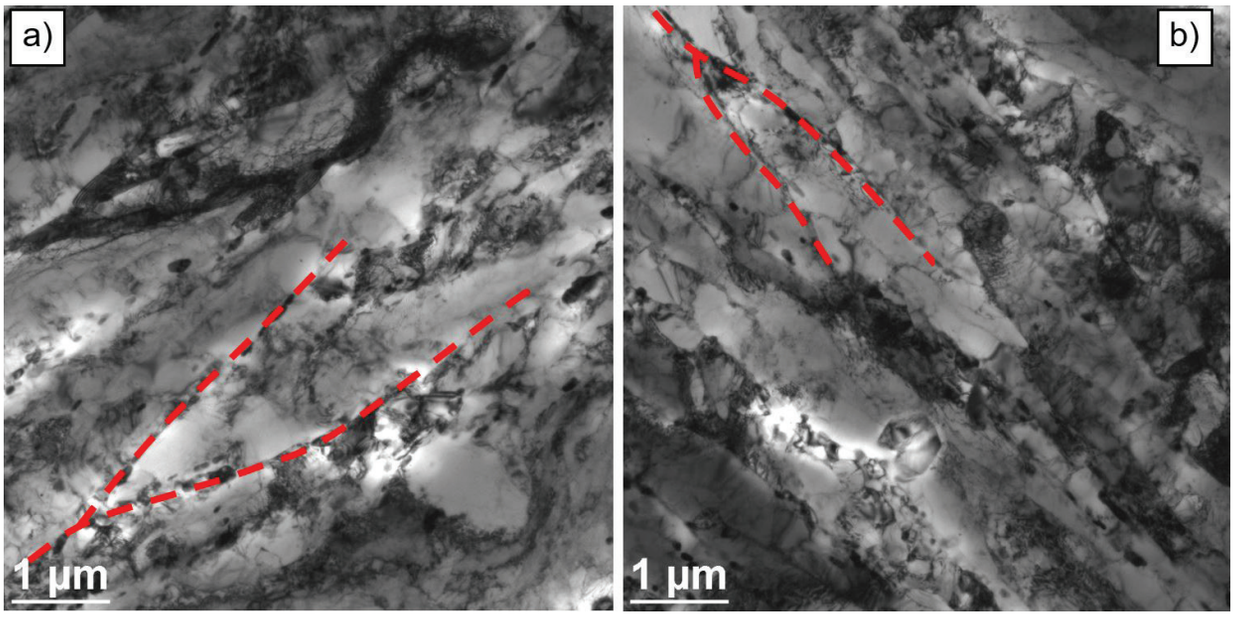

Figure 5. The morphology of "Y" nodes in: (a) P91, (b) PB2, TEM [15].

in martensitic steels is 50–150 nm [8, 21]. The long-term service/aging contributes to changing the morphology of $M_{23}C_6$ carbides. These precipitates show a high tendency to coagulation. The process of coagulation of precipitates is determined by two basic factors: the thermodynamic and the kinetic one. The thermodynamic factor results from a large value of the surface energy of the interphase boundaries. As a result of coagulation, the surface energy decreases and aims at reaching the energy equilibrium. The kinetic factor of coagulation, on the other hand, is connected with the diffusion and reactions occurring on the boundary surface. They run at different rates, and the slowest one determines the rate of particle growth in the system, and thereby determines the kinetics of coagulation. The constant of the rate of growth of particles K_p in the matrix of martensitic steels is presented in **Table 1**.

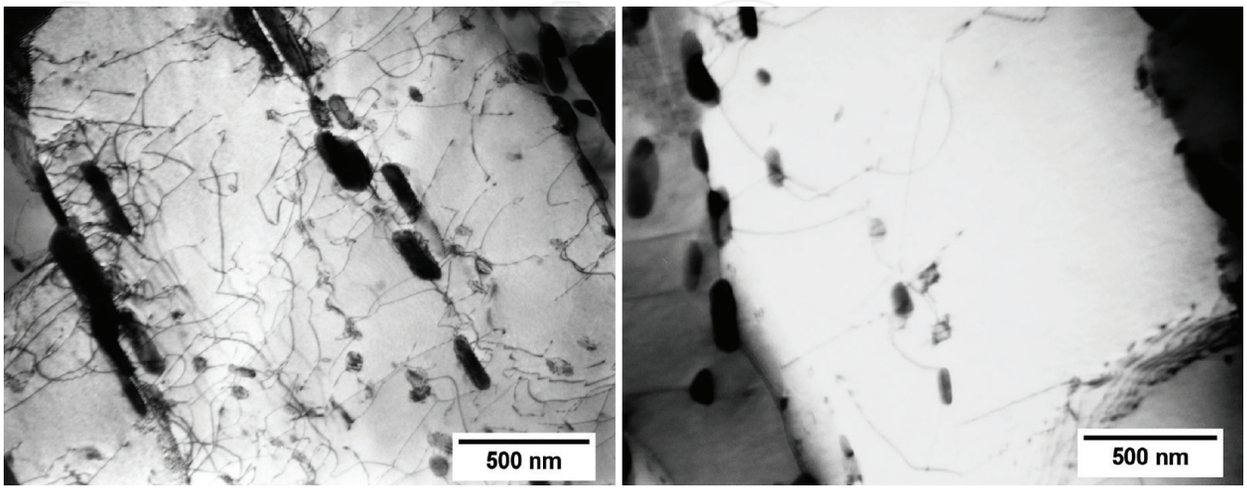

Figure 6. The interaction of dislocations in GP91 cast steel with particles of precipitates occurred after low-cycle fatigue.

http://dx.doi.org/10.5772/intechopen.70552

Precipitate	Steel	Temperature, °C	Based on solubilities at tempering temperature		Based on solubilities at exposure temperature	
			K_p, $m^3\ s^{-1}$	γ, J/m^2	K_p, $m^3\ s^{-1}$	γ, J/m^2
MX	P92	600	1.17×10^{-32}	0.5	8.58×10^{-33}	0.5
		650	9.5×10^{-32}	0.5	65.5×10^{-33}	0.5
Laves phase	P92	600	–	–	2.91×10^{-31}	1.0
		650			41.6×10^{-31}	1.0
$M_{23}C_6$	P92	600	0.12×10^{-29}	0.1	1.88×10^{-30}	0.1
		650	1.37×10^{-29}	0.1	4.78×10^{-30}	0.1
	P91	600	2.88×10^{-29}	1.0	7.67×10^{-30}	0.5
		650	25.3×10^{-29}	0.8	59.8×10^{-30}	0.3

Table 1. Calculated coarsening rate constants K_p of MX, Laves phase, and $M_{23}C_6$ precipitated in P91 and P92 steel based on the shown fit values for the interfacial energy γ [22].

The coagulation of $M_{23}C_6$ carbides reduces their amount with almost the same volume fraction and results in the increase in distance between these precipitates. Also, nonuniform distribution of these precipitates within matrix makes them become a less effective factor controlling the increase in the size of subgrains (**Figure 7**). The literature data [23] show that the subgrain boundaries with mutual disorientation angle of less than 20° are not the points of preferential carbide precipitation. According to the research in [24], only about 8% of $M_{23}C_6$ carbides was precipitated at the low-angle boundaries with mutual disorientation angle of 8–15°. The low-angle boundaries represent at least 60% of the total amount of boundaries in

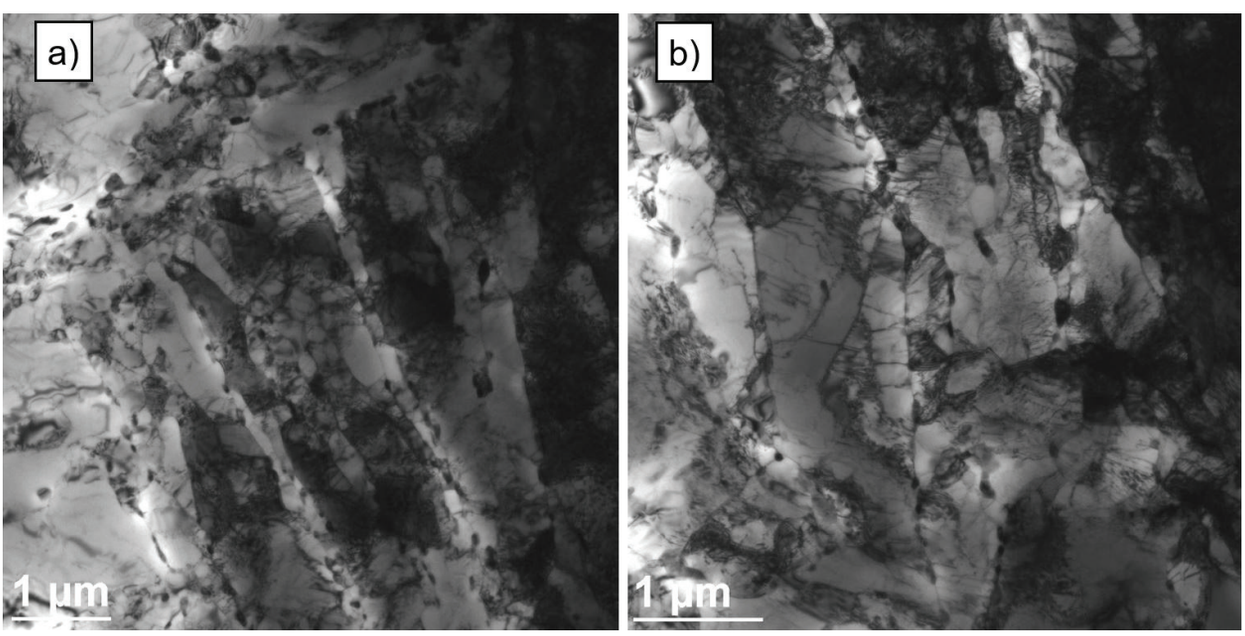

Figure 7. The microstructure of martensitic steels with both wide and narrow martensite laths visible: (a) P91, (b) PB2, TEM.

tempered martensite. This limits their role and reduces their effectiveness as a substructure stabilizer, which results in the reduction in creep strength. The precipitate-free boundaries show higher mobility, which results in an increase in their width. The increase in the size of $M_{23}C_6$ carbides precipitated at the boundaries is also conducive to the reduction in ductility of 9–12%Cr steels [6, 8, 22–26].

In steel with micro-addition of boron, the carbon atoms in $M_{23}C_6$ carbides are partially replaced by boron during the tempering, which results in the formation of $M_{23}(C, B)_6$ carboborides. Like $M_{23}C_6$ carbides, these precipitates occur at the grain boundaries and at the martensite lath boundaries. However, these precipitates are more finely dispersed and characterized by higher thermodynamic stability compared to $M_{23}C_6$ carbides [9, 14, 27]. This results in a slower increase in the size of these precipitates, which has a positive effect on the stability of tempered martensite lath microstructure and results in a higher creep resistance. Also according to [24], vanadium plays a significant role as a factor controlling the process of coagulation of $M_{23}C_6$ carbides. Vanadium dissolved in the matrix is conducive to decreasing of the coefficient of chromium diffusion in ferrite. Similar influence is also observed in the case of tantalum [28]. The temperature of work has a considerable effect on the rate of coagulation of $M_{23}C_6$ carbides. Elevating the temperature of service by 50°C can cause a growth of the rate of coagulation of these precipitates even by an order of magnitude.

The martensitic steels gain high creep resistance mainly due to the precipitation hardening provided by: MX nitrides, carbonitrides (where: M = V, Nb; X = C, N). MX precipitates are characterized by nanometric dimensions of about 10–50 nm, and in spite of their low volume fraction of 0.020–0.025, they ensure very strong hardening of creep-resistant steels (**Figure 8**).

The hardening with these precipitates is ensured by anchoring and hindering the motion of dislocations [6, 7, 9, 14, 15, 18, 29]. The calculations made for the P91 steel showed that the stress required for dislocation to "bypass" the carbide and nitride particles with the Orowan mechanism is as follows: for $M_{23}C_6$—39 MPa, for NbC—15 MPa, and for VN—106 MPa [30]. The MX precipitates in 9%Cr steels have a very high thermal stability (**Table 1**). The approximate formation enthalpy for these precipitates is as follows: for VC and NbC carbides, 55 and 70 kJ/mol, respectively, and for VN nitride, 125 kJ/mol [19]. High stability of MX precipitates and their coherent (semi-coherent) interphase boundaries cause that after approx. 100,000 h creep at 600°C, their size is similar to that as in the as-received condition [24, 30, 31].

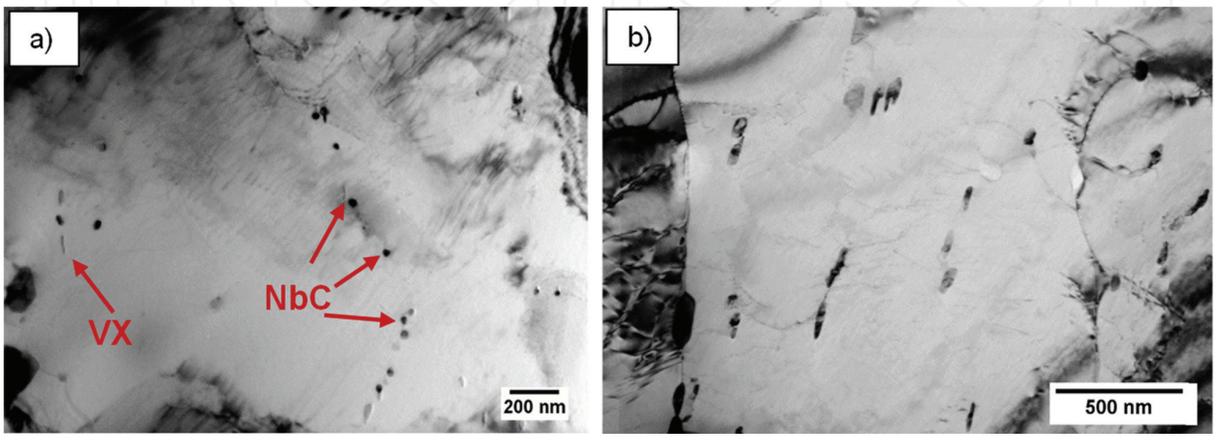

Figure 8. The MX precipitates in T91 steel after service: (a) NbC and VX, (b) V-wings [12].

http://dx.doi.org/10.5772/intechopen.70552

In martensitic steels used at above 600°C and containing at least 10%Cr, MX precipitates represent a metastable phase and undergo a transition into a more thermodynamically stable Z-phase (**Figure 9a**) [30–34]. The disappearance of finely dispersed MX precipitates in the microstructure of these steels due to the MX carbide → Z-phase transition (complex Cr(V, Nb)N nitride) results in a very fast decrease in creep resistance [31, 32, 34, 35].

According to [32, 35], one large Z-phase precipitate is formed at the expense of dissolving approx. 1000–1500 finely dispersed MX precipitates in the matrix. The disappearance of MX precipitates in martensitic steels during service in favor of Z-phase eliminates the effect of precipitation hardening with these particles. Nevertheless, as shown in [12], the interaction of MX precipitates with dislocations (**Figure 9b**) is still observed in the microstructure of P91 steel after service, and single Z-phase precipitates do not adversely affect its properties, and thus the creep strength (**Figure 10**).

Unlike the MX precipitates, both the chemical composition and the size of Z-phase depend on chemical composition of the steel it precipitates in and on creep duration. The Z-phase in 9%Cr steels is approx. 80–100 nm, whereas in steels with 11–12%Cr it is much larger and amounts to approx. 0.5–2 μm. Consequently, in 9%Cr steels the Z-phase precipitation is accompanied by a slight reduction in the volume fraction of MX precipitates, whereas in 12%Cr steels MX precipitates are virtually completely transformed into this complex nitride [31, 32, 36]. In addition, in 9%Cr steels the Z-phase precipitates after approx. 10^5 h at the earliest, while in 12%Cr steels the precipitation of this phase can be observed as early as after 10^3 h. Hence, the effect of Z-phase precipitates on creep strength is slight in steels with 9%Cr, whereas in 12%Cr steels it is significant [25, 32, 35, 36].

In high-chromium martensitic steels, the Z-phase precipitation may proceed with two mechanisms [32, 33]. The schematic transition of MX precipitates into Z-phase in high-chromium martensitic steels is shown in **Figure 11**.

On the other hand, dissolving NbX precipitates in the matrix "releases" carbon atoms, which results in the precipitation of chromium-rich $M_{23}C_6$ carbides, frequently nearby the Z-phase particles. The precipitation of Z phase is preferential near the grain boundaries of prior austenite, and in the steels containing delta ferrite additionally also near the interphase boundary mar-

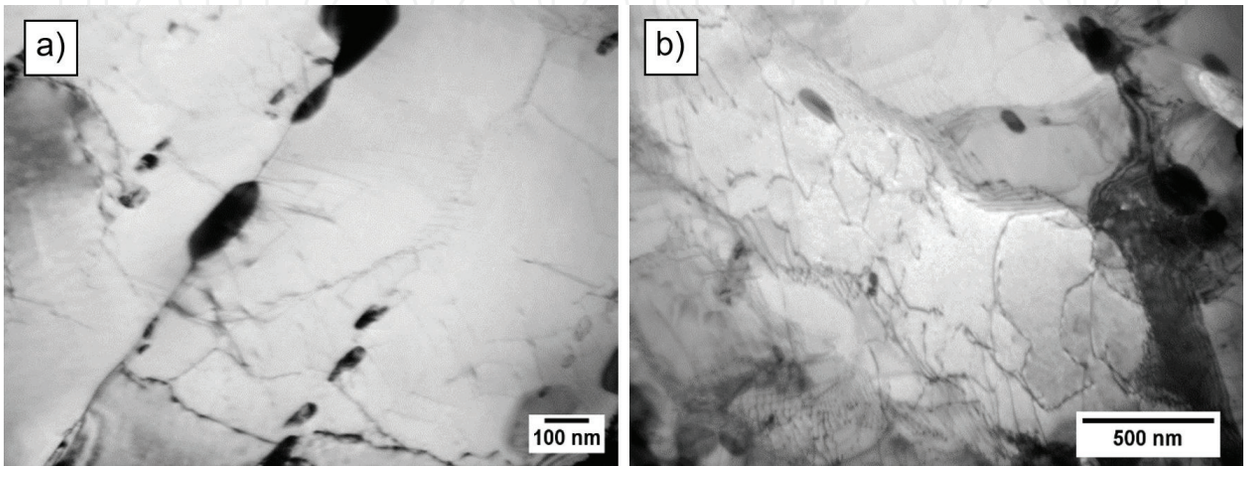

Figure 9. Z-phase precipitate in T91 steel after service (a), interaction of dislocations inside the subgrain with MX precipitates (b).

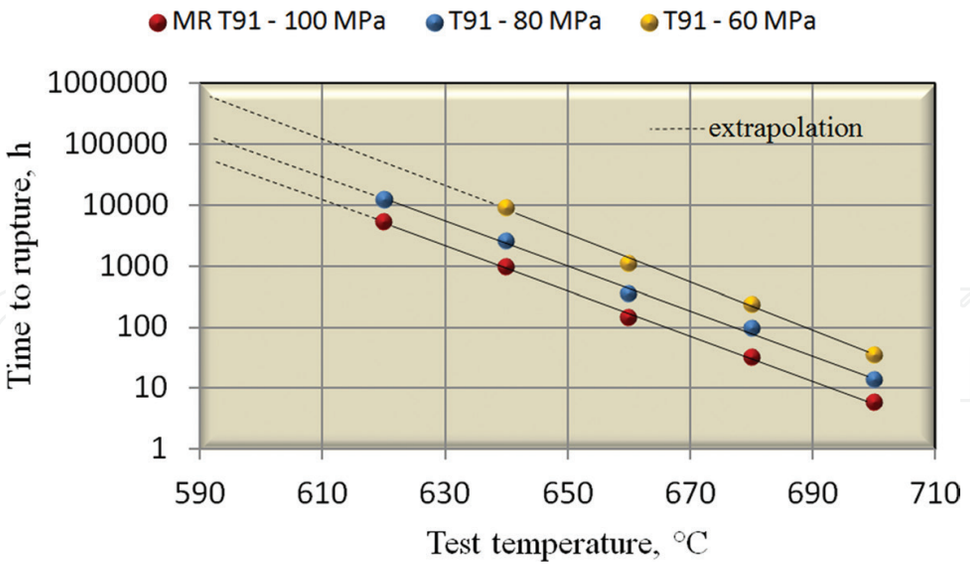

Figure 10. Results of short-term creep tests of T91 steel after service [12].

tensite/delta ferrite [14, 25, 33, 35, 36]. This is due to faster diffusion of substitution elements nearby these defects. It results in the formation of near-boundary areas free from MX precipitates, which leads to the accelerated matrix recrystallization and reduction in strength properties in these areas. Such changes lead to the formation of creep grain, which is unequal in volume, and consequently to a faster destruction of steel during service [32, 35, 36]. The disappearance of

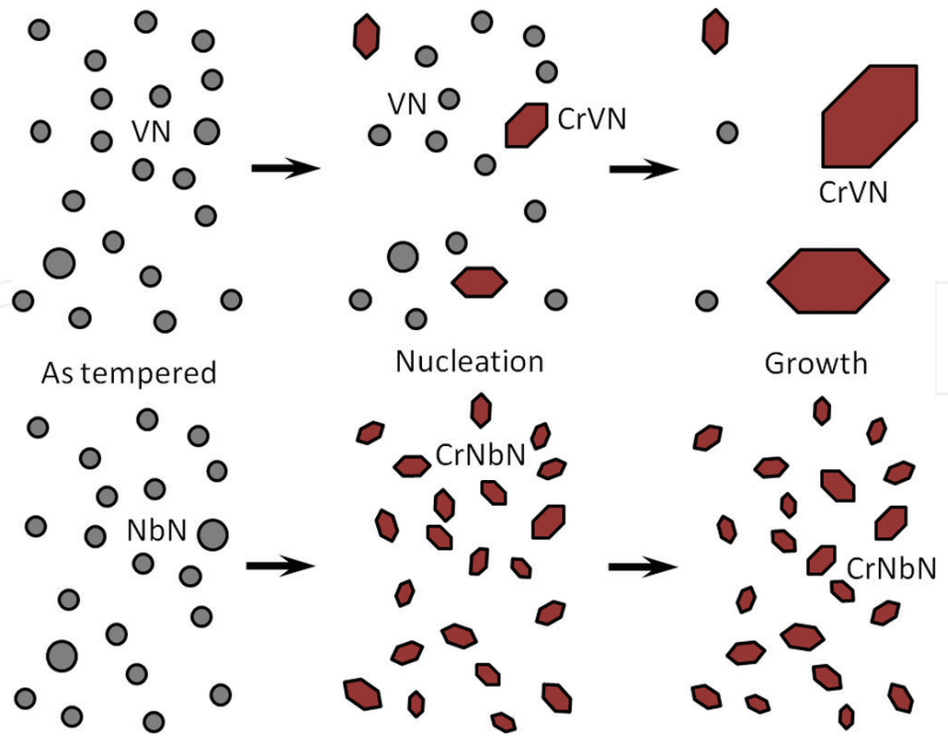

Figure 11. Schematic transition of MX precipitates into Z-phase [32].

finely dispersed MX precipitates also results in disproportionately high reduction in hardness in relation to other mechanical properties [21].

In martensitic steels containing approx. 9%Cr, a more important problem is the increase in the size of $M_{23}C_6$ carbides as well as the precipitation and growth of intermetallic Fe_2Mo Laves phase [6, 7, 25, 37]. In 9–12%Cr steels in the as-received condition, the Laves phase does not occur. The precipitation of this phase takes place during service/aging mainly at the grain/lath boundaries, frequently nearby $M_{23}C_6$ carbides **Figure 12** [37–39]. In the case when the total content of W + Mo in the steel amounts to at least 4.53, the particles of Laves phase precipitate heterogeneously at grain boundaries as well as homogeneously within grains, forming the precipitation free zone on both sides of the grain boundary [40].

It is assumed that due to high dispersion in the initial period of the precipitation the Laves phase has a positive effect on properties of these steels by increasing the precipitation hardening. However, low stability of the Laves phase results in its high coagulability, which results in a very fast increase in its size [15, 25, 37, 39].

The Laves phase precipitating in 9–12%Cr creep-resistant steels makes the matrix deplete of substitution elements (tungsten, molybdenum, chromium), which increases the tendency of these steels to the recovery and polygonization process and reduces their resistance to oxidation. On the other hand, the matrix depletion of substitution elements (Cr, Mo, W), which are also components of $M_{23}C_6$ carbides, has a positive effect on the inhibition of coagulation of these precipitates [12, 38]. According to [41, 42], the nucleation and growth of Laves phase requires the enrichment of micrograin boundaries not only in Mo and Si, but also in phosphorus.

The Laves phase precipitates with average diameter above 130 nm also contribute to the change in cracking mechanism from ductile to brittle (transcrystalline, cleavable fracture) and are the main reason for sudden reduction in creep strength of [40, 41, 43, 44]. The Laves phase and $M_{23}C_6$ carbide precipitates occurring during long-term service form the so-called continuous grid of precipitates at the grain boundaries (**Figure 13**), which contributes to a decrease in ductility of 9% Cr steel [8, 12, 43–49].

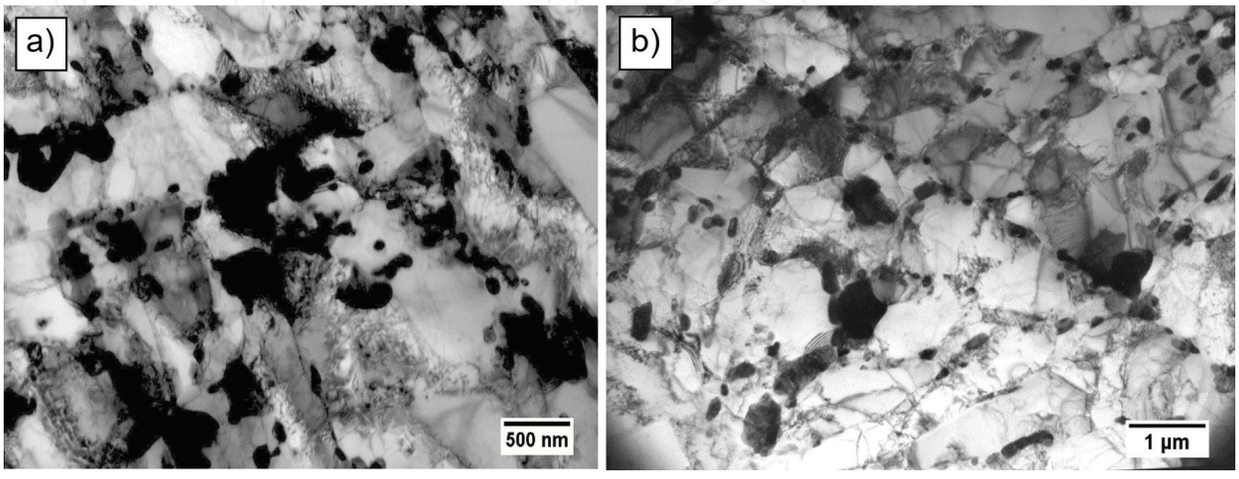

Figure 12. Precipitation of Laves phase at the grain boundary nearby $M_{23}C_6$ carbides: (a) T91 steel, (b) GP91 cast steel [38].

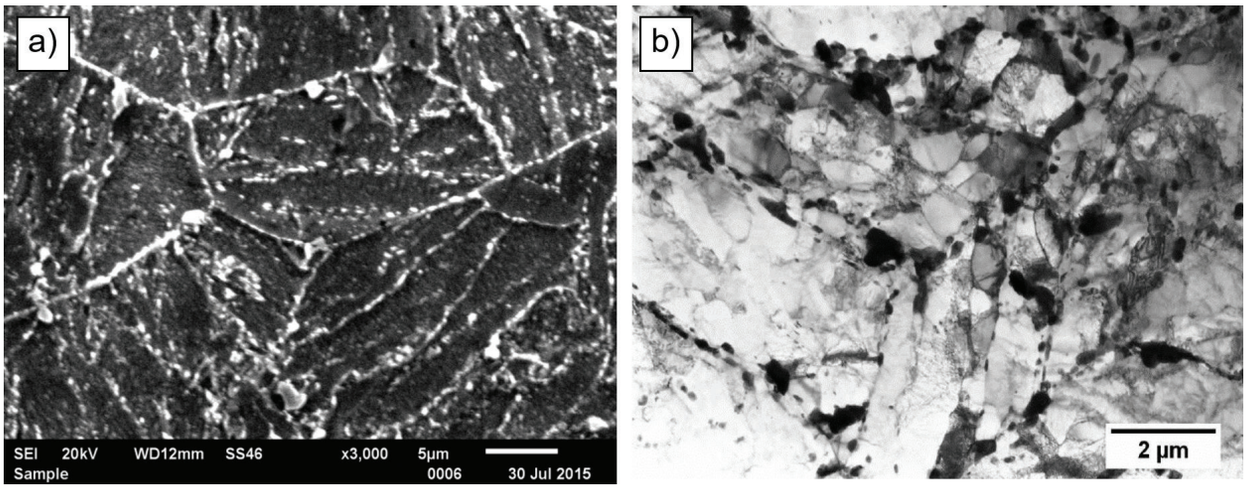

Figure 13. Continuous grid of precipitates at the former austenite grain boundaries (a) P91 steel (SEM), (b) GP91 cast steel (TEM) [49].

The increase in stability of the Laves phase precipitates in these steels can be achieved by the addition of boron and/or tungsten [50, 51]. On the contrary, phosphorus, silicon, and cobalt have an adverse effect as they stimulate the precipitation of the Laves phase [52, 53].

In the tempered structure of martensite in steel of the 9–12%Cr type, in the case of the typical volume fractions of particular precipitates and spacing between them, the Orowan stress can be estimated as shown in **Table 2**.

The precipitation processes as well as the growth of carbides and secondary phases, which occurs during the operation of creep-resistant steels, make the matrix deplete of substitution elements as a result of their diffusion into these precipitates.

The matrix depletion of the above-mentioned elements facilitates the self-diffusion processes, speeds up the matrix recovery and polygonization processes, and reduces the oxidation resistance, thus contributing to the reduction in high-temperature creep resistance and life of these steels [11, 54].

An important factor affecting the basic property of 9–12%Cr steels, i.e., creep strength, is aluminum content in the steel. The addition of aluminum to steel is to deoxide it in the metallurgical process, hence part of aluminum will remain as Al_2O_3 in the steel, while the other part in the atomic form is dissolved in solid solution. The aluminum content in 9–12%Cr steels for

Particle	Volume fraction, %	Diameter, nm	Spacing, nm	Orowan stress, MPa
Fe_2M	1.5	70	410	95
$M_{23}C_6$	2	50	260	150
MX	0.2	20	320	120

Table 2. Volume fraction, diameter, and spacing of each kind of precipitates in high-chromium martensitic steel, together with Orowan stress from the values of interparticle spacing [14].

http://dx.doi.org/10.5772/intechopen.70552

the power industry should not exceed 0.04%. Due to its greater affinity to nitrogen, aluminum forms large lamellar AlN nitrides of about 0.5–1.0 μm to prevent the formation of finely dispersed vanadium-rich MX precipitates. This results in not only a reduction in the volume fraction of vanadium-rich MX precipitates, but also in a change in their chemical composition. There occurs a decrease in the amounts of vanadium and nitrogen with simultaneous increase in the amounts of niobium and carbon in these precipitates, which makes niobium-rich carbides (NbC) become the main precipitate in martensitic steel. This results in a decrease in creep strength of martensitic steels: for P91—by about 10% at 600°C, whereas for P92 the time to rupture of test specimen was shorter by 7–30 times, depending on test temperature and stress [30, 55]. Higher than permissible aluminum content in 9–12%Cr steels has a positive

Features of microstructure		**As-received condition**	**Creep/aging**
Matrix	Dislocation density	High	Low/very low
	Size, width of subgrains/ martensite laths	High-temperature tempered martensite microstructure with small width of laths	Recovery and polygonization process – transformation of the lath martensite microstructure into the polygonised ferrite grain microstructure
Precipitates	MX	Finely dispersed (~20–50 nm), precipitated inside laths at dislocations, limit grain growth, make steel precipitation-hardened	Finely dispersed (~20–50 nm), precipitated inside laths at dislocations, limit grain growth, make steel precipitation-hardened, change into Z-phase
	$M_{23}C_6$	50–150 nm, precipitated at the martensite lath boundaries and at the former austenite grain boundaries, stabilize substructure	≥220 nm, partially precipitated at the subgrain boundaries, coagulate during creep/ aging resulting in a reduction in creep strength and increase in embrittlement
	Z-phase	Nonexistent	Formed at the expense of finely dispersed MX precipitates, causes sudden decrease in creep strength
	Laves phase	nonexistent	Medium and large size of precipitates (≥0.5–1 μm), precipitated at the grain and subgrain boundaries nearby $M_{23}C_6$, decreases creep strength and reduces ductility

Table 3. Basic features of microstructure in 9–12%Cr steels in the as-received condition and after creep.

effect on the increase in impact strength and reduction in brittle fracture appearance transition temperature, which is the result of positive effect of AlN on the austenite grain refinement. The increase in aluminum content from 0.03 to 0.094% in P92 steel makes the average diameter of austenite grain decrease from 50 μm (which corresponds to the grain grade of 5.5) to 10 μm (grain grade 10) [30, 56]. The negative impact of aluminum on creep resistance requires control of chemical composition of 9–12%Cr steel as early as at its production stage, in particular with regard to elements with high affinity to nitrogen, such as Al and Ti, so as to prevent from the formation of unfavorable AlN or TiN nitrides at the expense of finely dispersed VN precipitates.

The basic features of the microstructure of 9–12%Cr steel in the as-received condition and after long-term service/aging are summarized in **Table 3**.

Author details

Grzegorz Golański*, Cezary Kolan and Joanna Jasak

*Address all correspondence to: grisza@wip.pcz.pl

Institute of Materials Engineering, Czestochowa University of Technology, Czestochowa, Poland

References

[1] Viswanathan R, Bakker W. Materials for ultrasupercritical coal power plants—Boiler materials—Part 1. Journal of Materials Engineering and Performance. 2001;**10**:81-95. DOI:10.1361/105994901770345394

[2] Masuyama F. History of power plants and progress in heat resistant steels. ISIJ International. 2001;**41**:612-625. DOI: 10.2355/isijinternational

[3] Bhadeshia HKDH. Design of ferritic creep-resistant steels. ISIJ International. 2001;**41**:626-640. DOI: 10.2355/isijinternational

[4] Golański G, Stachura S. Characterization of new-low alloy steels for power plant. Hutnik–Wiadomości Hutnicze. 2009;**9**:679-683 (in Polish)

[5] Abe F. New martensitic steels. In: Di Gianfrancesco A, editor Materials for Ultra-Supercritical and Advanced Ultra-Supercritical Power Plants. Woodhead Publishing; 2017. pp. 323-374

[6] Panait CG, Bendick W, Fuchsmann A, Gourgues-Lorenzon AF, Besson J. Study of the microstructure of the grade 91 steel after more than 100,000 h of creep exposure at 600°C. International Journal of Pressure Vessels and Piping. 2010;**87**:326-335. DOI: 10.1016/j.ijpvp.2010.03.017

[7] Panait CG, Zielińska-Lipiec A, Kozieł T, Czyrska-Filemonowicz A, Gourgues-Lorenzon AF, Bendick W. Evolution of dislocation density, size of subgrains and MX-type precipitates in a P91 steel during creep and during thermal ageing at 600°C for more than 100,000 h. Materials Science and Engineering. 2010;**527A**:4062-4069. DOI: 10.1016/j.msea.2010.03.010

[8] Golański G, Mroziński S. Low cycle fatigue and cyclic softening behaviour of martensitic cast steel. Engineering Failure Analysis. 2013;**35**:692-702. DOI: 10.1016/j.engfailanal.2013.06.019

[9] Dudova N, Mishnev R, Kaibyshev R. Effect of tempering on microstructure and mechanical properties of boron containing 10% Cr steel. ISIJ International. 2011;**51**:1912-1918. DOI: 10.2355/isijinternational

[10] Baek JH, Kim SH, Lee CB, Hahn DH. Mechanical properties and microstructural evolution of modified 9Cr-1Mo steel after long-term aging for 50,000 h. Metals and Materials International. 2009;**15**:565-573. DOI: 10.1007/s12540-009-0565-y

[11] Qiang L. Modeling the microstructure–mechanical property relationship for a 12Cr–2W–V–Mo–Ni power plant steel. Materials Science and Engineering. 2003;**361A**:385-391. DOI: 10.1016/S0921-5093(03)00565-3

[12] Golański G, Zielińska-Lipiec A, Zieliński A, Sroka M. Effect of long-term on microstructure and mechanical properties of martensitic 9%Cr steel. Journal of Materials Engineering and Performance. 2017;**26**:1101-1107

[13] Golański G. Evolution of secondary phases in GX12CrMoVNbN9-1 cast steel after heat treatment. Archives of Materials Science and Engineering. 2011;**48**:12-18

[14] Abe F. Precipitate design for creep strengthening of 9% Cr tempered martensitic steel for ultra-supercritical power plants. Science and Technology of Advanced Materials. 2008;**9**:1-15. DOI: 10.1088/1468-6996/9/1/013002

[15] Golański G, Jasak J, Zieliński A, Wieczorek P. Quantitative analysis of stability of 9%Cr steel microstructure after long-term ageing. Archives of Metallurgy and Materials. 2017;**62**:273-281. DOI: 10.1515/AMM-2017-0040

[16] Ghassemi-Armaki H, Chen RP, Maruyama K, Yoshizawa M, Igarashi M. Static recovery of tempered lath martensite microstructures during long-term aging in 9-12%Cr heat resistant steels. Materials Letters. 2009;**63**:2423-2425. DOI: 10.1016/j.matlet.2009.08.024

[17] Abe F. Coarsening behavior of lath and its effect on creep rates in martensitic 9Cr–W steels. Materials Science and Engineering. 2004;**387-389A**:565-569. DOI: 10.1016/j.msea.2004.01.057

[18] Xu LQ, Zhang DT, Liu YC, Ning BQ, Qiao ZX, Yan ZS, Li HJ. Precipitation behavior and martensite lath coarsening during tempering of T/P92ferritic heat-resistant steel. International Journal of Minerals, Metallurgy, and Materials. 2014;**21**:438-447. DOI: 10.1007/s12613-014-0927-4

[19] Nes E, Ryum N, Hunderi O. On the Zener drag. Acta Metallurgica. 1985;**33**:11-22. DOI: 10.1016/0001-6160(85)90214-7

[20] Pickering FB. Historical development and microstructure of high chromium ferritic steels for high temperature applications. In: Strang A, Gooch DJ, editors. Microstructural Development and Stability in High Chromium Ferritic Power Plant Steels. London: The Institute of Materials Cambridge; 1997. pp. 1-29

[21] Kadoya Y, Dyson BF, McLean M. Microstructural stability during creep of Mo- or W-bearing 12Cr steels. Metallurgical and Materials Transactions. 2002;**33A**:2549-2557. DOI: 10.1007/s11661-002-0375-z

[22] Hald J, Korcakova L. Precipitate stability in creep resistant ferritic steels—Experimental investigation and modelling. ISIJ International. 2003;**43**:420-427. DOI: 10.2355/isijinternational

[23] Laws MS, Goodhew PJ. Grain boundary structure and chromium segregation in a 316 stainless steel. Acta Metallurgica. 1991;**39**:1525-1533. DOI: 10.1016/0956-7151(91)90238-V

[24] Xu Y, Zhang X, Tian Y, Chen C, Nan Y, He H. Wang M. Study on the nucleation and growth of $M_{23}C_6$ carbides in a 10% Cr martensite ferritic steel after long-term aging. Materials Characterization. 2016;**111**:122-127. DOI: 10.1016/j.matchar.2015.11.023

[25] Golański G, Zieliński A, Słania J, Jasak J. Mechanical properties of VM12 steel after 30 000 hrs of ageing at 600°C temperature. Archives of Metallurgy and Materials. 2014;**59**:1351-1354. DOI: 10.2478/amm-2014-0230

[26] Yan W, Wang W, Shan YY, Yang K. Microstructural stability of 9-12%Cr ferrite/martensite heat-resistant steels. Frontiers of Materials Science. 2013;**7**:1-27. DOI: 10.1007/s11706-013-0189-5

[27] Abe F, Horiuchi T, Taneike M, Sawada K. Stabilization of martensitic microstructure in advanced 9Cr steel during creep at high temperature. Materials and Science Engineering. 2004;**378A**:299-303. DOI: 10.1016/j.msea.2003.11.073

[28] Xiao X, Liu G, Hu B, Wang J, Ma W. Coarsening behawior for M23C6 carbide in 12%Cr-reduced activation ferrite/martensite steel: Experimental study combined with DICTRA simulation Journal of Materials Science. 2013;**48**:5410-5419. DOI: 10.1007/s10853-013-7334-5

[29] Abe F, Taneike M, Sawada K. Alloy design of creep resistant 9Cr steel using a dispersion of nano-sized carbonitrides. International Journal of Pressure Vessels and Piping. 2007;**84**:3-12. DOI: 10.1016/j.ijpvp.2006.09.003

[30] Magnusson H, Sandström R. Influence of aluminium on creep strength of 9-12% Cr steel. Materials Science and Engineering. 2009;**527A**:118-125. DOI: 10.1016/j.msea.2009.07.060

[31] Danielsen HK, Hald J. Behaviour of Z phase in 9-12%Cr steels. Energy Materials. 2006;**1**:49-57. DOI: 10.1179/174892306X99732

[32] Danielsen HK. Precipitation process of Z-phase in 9-12%Cr steels, In: Gandy A, Shingledecker J, editors. Advances in Materials Technology for Fossil Power Plants. 7th International Conference, Waikoloa, Hawaii, USA. 2013: pp. 1104-1115.

[33] Golpayegani A, Andrén HO, Danielsen HK, Hald J. A study on Z–phase nucleation in martensitic chromium steels. Materials Science and Engineering. 2008;**489A**:310-318. DOI: 10.1016/j.msea.2007.12.022

[34] Sawada K, Kushima H, Kimura K, Tabuchi M. TTP diagrams of Z phase in 9-12%Cr heat-resistant steels. ISIJ International. 2007;**47**:733-739. DOI: 10.2355/isijinternational

[35] Sawada K, Kushima H, Kimura K, Tabuchi M. Z-phase formation and its effect on long-term creep strength in 9-12%Cr creep resistant steels. Transactions of the Indian Institute of Metals. 2010;**63**:117-122. DOI: 10.1007/s12666-010-0016-y

[36] Yoshizawa M, Igarashi M, Moriguchi K, Iseda A, Armaki HG, Maruyama K. Effect of precipitates on long-term creep deformation properties of P92 and P122 type advanced ferritic steels for USC power plants. Materials Science and Engineering. 2009;**510-511A**: 162-168. DOI: 10.1016/j.msea.2008.05.055

[37] Li Q. Precipitation of Fe_2W laves-phase and modeling of its direct influence on the strength of a 12Cr-2W steel. Metallurgical and Materials Transactions. 2006;**37A**:89-97. DOI: 10.1007/s11661-006-0155-2

[38] Golański G, Zielińska-Lipiec A, Mroziński S, Kolan C. Microstructural evolution of aged heat resistant cast steel following strain controlled fatigue. Materials Science and Engineering. 2015;**627A**:106-110. DOI: 10.1016/j.msea.2014.12.120

[39] Aghajani A, Richter F, Somsen C, Fries S, Steinbach I, Eggeler G. On the formation and growth of Mo–Rich laves phase particles during long-term creep of a 12% chromium tempered martensite ferritic steels. Scripta Materialia. 2009;**61**:1068-1071. DOI: 10.1016/j.scriptamat.2009.08.031

[40] Zhu S, Yang M, Song XL, Zhang Z, Wang LB, Tang S, Xiang ZD. A few observations on laves phase precipitation in relation to its effects on creep rupture strength of ferritic steels based on Fe-9Cr(wt%) alloys at 650°C. Materials Science and Engineering. 2014;**619A**:47-56. DOI: 10.1016/j.msea.2014.09.059

[41] Isik MI, Kostka A, Eggeler G. On the nucleation of laves phase particles during high-temperature exposure and creep of tempered martensite ferritic steels. Acta Materialia. 2014;**81**:230-240. DOI: 10.1016/j.actamat.2014.08.008

[42] Isik MI, Kostka A, Yardley VA, Pradeep KG, Duarte MJ, Choi PP, Raabe D, Eggeler G. The nucleation of Mo-rich laves phase particles adjacent to $M_{23}C_6$ micrograin boundary carbides in 12%Cr tempered martensite ferritic steels. Acta Materialia. 2015;**90**:94-104. DOI: 10.1016/j.actamat.2015.01.027

[43] Zieliński A, Golański G, Sroka M, Tański T. Influence of long-term service on microstructure, mechanical properties, and service life of HCM12A steel. Materials at High Temperatures. 2016;**33**:24-32. DOI: 10.1179/1878641315Y.0000000015

[44] Lee JS, Armaki HG, Maruyama K, Muraki T, Asahi H. Causes of breakdown of creep strength in 9Cr-1.8W-0.5Mo-VNb steel. Materials Science and Engineering. 2006;**428A**:270-275. DOI: 10.1016/j.msea.2006.05.010

[45] Zieliński A, Golański G, Sroka M. Assessment of microstructure stability and mechanical properties of X10CrWMoVNb9-2 (P92) steel after long-term thermal ageing for high-temperature applications. Kovove Materialy. 2016;**56**:61-70. DOI: 10.4149/km-2016-1-61

[46] Zieliński A, Dobrzański J, Purzyńska H, Golański G. Changes in properties and microstructure of high-chromium 9-12%Cr steels due to long–term exposure at elevated temperature. Archives of Metallurgy and Materials. 2016;**61**:957-964. DOI: 10.1515/amm-2016-0163

[47] Paul VT, Soraja S, Vijayalakshmi M. Microstructural stability of modified 9Cr–1Mo steel during long term exposures at elevated temperatures. Journal of Nuclear Materials. 2008;**378**:273-281. DOI: 10.1016/j.jnucmat.2008.06.033

[48] Yan P, Liu Z. Toughness evolution of 9Cr-3W-3Co martensitic heat resistant steel during long time aging. Materials Science and Engineering. 2016;**650A**:290-294. DOI: 10.1016/j.msea.2015.09.115

[49] Golański G, Kępa J. The influence of ageing temperatures on microstructure and mechanical properties of GX12CrMoVNb9-1 (GP91) cast steel. Archives of Metallurgy and Materials. 2012;**57**:757-582. DOI: 10.2478/v10172-012-0061-0

[50] Park JS, Kim SJ, Lee CS. Effect of W addition on low cycle fatigue behavior of high Cr ferritic steels. Materials Science and Engineering. 2001;**298A**:127-136. DOI: 10.1016/S0921-5093(00)01291-0

[51] Artinger I, Elarbi Y. Effect of aging time and boron addition on the properties of 9-12%Cr power plant steels—Outcomes from different experimental investigations. Periodica polytechnical/Mechanical Engineering. 2006;**50**:3-10

[52] Yamada K, Igarashi M, Muneki S, Abe F. Effect of co addition on microstructure in high Cr ferritic steels. ISIJ International. 2003;**43**:1438-1443. DOI: 10.2355/isijinternational.43.1438

[53] Helis L, Toda Y, Hara T, Miyazaki H, Abe F. Effect of cobalt on the microstructure of tempered martensitic 9Cr steel for ultra-supercritical power plants. Materials Science and Engineering. 2009;**510-511A**:88-94. DOI: 10.1016/j.msea.2008.04.131

[54] Maruyama K, Sawada K, Koike J. Strengthening mechanisms of creep resistant tempered martensitic steel. ISIJ International. 2001;**41**:641-653. DOI: 10.2355/isijinternational

[55] Naoi H, Ohgami M, Liu X, Fujita T. Effects of aluminium content on the mechanical properties of a 9Cr–0.5Mo–1.8W steel. Metallurgical and Materials Transactions. 1997;**28A**:1195-1203. DOI: 10.1007/s11661-997-0284-2

[56] Foldyna V, Jakobová A, Riman R, Gemperle A. Effects of structural factors on the creep properties of modified chromium steels. Steel Research International. 1991;**60**:453-458. DOI: 10.1002/srin.199100429